NIST-F3, a cesium fountain frequency reference

Gregory W. Hoth, Jeff A. Sherman, *National Institute of Standards and Technology*
Alexander G. Radnaev, Peter Mitchell, *Infleqtion, 3030 Sterling Circle, Boulder, CO 80301, USA*
Vladislav Gerginov *National Institute of Standards and Technology and University of Colorado Boulder*

BIOGRAPHY

Gregory W. Hoth. Greg is a physicist in the Time Realization and Distribution group at NIST. His work is focused on developing and maintaining the cesium fountains at NIST. He received his PhD from the University of Colorado Boulder in 2016.

Jeff A. Sherman. Jeff obtained a B.Sc. in Physics from the University of Texas at Austin and a Ph.D. in Physics from the University of Washington. Jeff is currently a research physicist at NIST focusing on time scale realization and distribution.

Alexander G. Radnaev. Dr. Alexander Radnaev received his PhD degree at Georgia Institute of Technology in 2012 demonstrating laser cooling of triply charged Thorium-229 towards optical nuclear clock and interfacing long-lived quantum memory with telecommunication fibers using single-photon level four-wave mixing in cold Rb vapor. After spending six years in the semiconductor, laser, and software industries he worked at NIST Time and Frequency division where he built the NIST-F3 physics package. He is currently leading development of a quantum computer at Infleqtion (previously ColdQuanta).

Peter Mitchell. Peter Mitchell received his BS in Engineering Physics at the University of Colorado Boulder in 2021. He assisted with the construction of the NIST-F3 physics package while at NIST Time and Frequency division and is currently a junior physicist working on the development of neutral atom quantum computing at Infleqtion (previously ColdQuanta).

Vladislav Gerginov. Dr. Vladislav Gerginov received his M.Sc. degree from Sofia University, Sofia, Bulgaria in 1995 and his PhD degree from the University of Notre Dame, IN, USA in 2003. He worked on the Primary Frequency Standard PTB-CSF2 at the Physikalisch-Technische Bundesanstalt (PTB, Germany) between 2008 and 2016. He presently works at the University of Colorado at Boulder and NIST, USA since 2019. His main research areas of interest are atomic physics and frequency metrology.

ABSTRACT

A cesium fountain frequency reference known as NIST-F3 is under development at the National Institute of Standards and Technology (NIST). The fountain is intended to provide input for the NIST timescale and assist with evaluation of NIST's primary and secondary frequency standards. Here, we describe details of the NIST-F3 apparatus and demonstrate a short-term frequency stability of $2.2 \times 10^{-13}/\sqrt{\tau}$ for averaging times as long as 5×10^4 s (τ is the averaging time in seconds). We also present an initial evaluation of the main frequency biases. Due to the particulars of the microwave cavity design employed in NIST-F3, the fountain exhibits a relatively large tilt sensitivity. We measure fractional frequency shifts of order $10^{-14}/\mathrm{mrad}$ when tilting the fountain. Despite this complication, we show that the tilt sensitivity can be managed with the standard techniques that have been developed for cold-atom fountains. This initial investigation suggests it will be possible to achieve our goal of a fractional frequency stability better than 0.5×10^{-15} for up to a few months of averaging time.

I. INTRODUCTION

Frequency references based on cold atoms can provide excellent long-term stability. Several timing laboratories have shown that this long-term frequency stability can be used to improve the stability of a local realization of Coordinated Universal Time (UTC) by incorporating signals from cold-atom fountains based on microwave transitions (Bauch et al., 2012; Rovera et al., 2016; Peil et al., 2016) or an optical lattice clock (Hachisu et al., 2018). The local realization of UTC maintained by the National Institute of Standards and Technology (NIST) does not currently receive input from a cold-atom frequency reference. In order to improve UTC(NIST), a new cesium fountain known as NIST-F3 is under development. Although it is based on cesium, this fountain is intended to operate as a frequency reference rather than a primary frequency standard. Once the fountain is operational, it will provide input to the NIST timescale and assist with evaluation of NIST's primary and secondary frequency standards. Quantitatively, we hope to achieve a fractional frequency stability better than 0.5×10^{-15} up to a few months of averaging time. In order to realize this goal, we need to understand, control, and monitor the largest frequency biases of NIST-F3, but we do not intend to achieve the state of the art in accuracy for a Cesium fountain where all frequency biases can be characterized with a combined systematic uncertainty of order 1×10^{-16} (Guéna et al., 2012; Levi et al., 2014; Heavner et al., 2014; Szymaniec et al., 2016; Weyers et al., 2018; Beattie et al., 2020).

In Section II, we describe some details of NIST-F3's physics package and present measurements of the short-term frequency

https://doi.org/10.33012/2023.18691

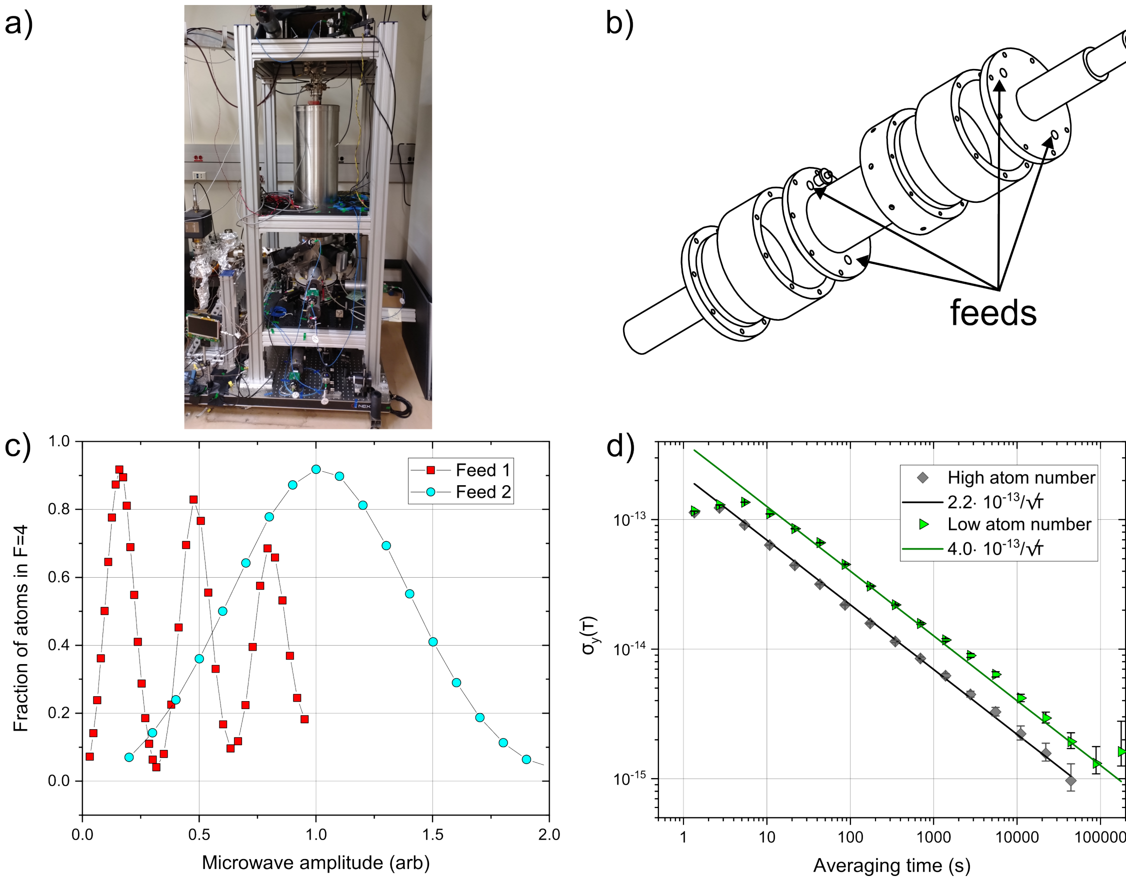

Figure 1: a) A photograph of NIST-F3's physics package. b) A schematic diagram of the microwave cavity assembly for NIST-F3. Both the state selection and the Ramsey cavities are shown. The arrows highlight the holes in the upper endcap of each cavity where microwaves are fed into the cavity. An antenna is shown above one feed in the lower cavity. c) Rabi oscillations observed when driving the Ramsey cavity with a single feed as a function of the input microwave amplitude. We see that one feed requires significantly more microwave power to drive the atoms from $|F = 3\rangle$ to $|F = 4\rangle$. The lines connecting adjacent points are a guide for the eye. d) Measured short-term frequency stability for NIST-F3 with two different atom numbers from a 14-day-run. The short-term stability is calculated with the overlapping Allan variance. During the run, the fountain alternates between high-density and low-density mode every few minutes.

stability. In Section III, we discuss the frequency biases that have been investigated so far in NIST-F3, which are the quadratic Zeeman shift, the gravitational redshift, the black body radiation (BBR) shift, the collisional shift, and the fountain's tilt sensitivity. The tilt sensitivity arises from phase gradients in the microwave cavity used for the Ramsey interrogation, and it is typically known as an $m = 1$ distributed cavity phase (DCP) error in the fountain literature (Khursheed et al., 1996; Li and Gibble, 2004, 2010; Guéna et al., 2011).

II. PHYSICS PACKAGE

In most respects, NIST-F3 is a typical Cesium fountain (Wynands and Weyers, 2005). Cesium atoms are cooled in an optical molasses at the bottom of the fountain with two pairs of horizontal laser beams and one pair of vertical laser beams. The atoms are launched upward to a height of approximately 0.78 m above the molasses zone (0.17 m above the Ramsey cavity) by introducing frequency shifts into the vertical molasses beams. After the launch, atoms in the $|F = 3, m = 0\rangle$ hyperfine state are isolated by use of a microwave pulse in the state selection cavity followed by a resonant laser pulse which removes the atoms in the $|F = 4\rangle$ state. Then, the selected atoms pass through a second microwave cavity which is used to realize Ramsey interrogation during the atoms' parabolic flight. The atomic state is detected at the end of the fountain sequence by collecting fluorescence from the atoms as they cross several resonant laser beams. In a typical shot of the experiment, we load the optical molasses for 0.5 s and allow 0.9 s for the fountain sequence. The Ramsey time is approximately 0.38 s, and we obtain Ramsey fringes with a width of 1.3 Hz (full width at half maximum). A photograph of the vacuum system is shown in Fig. 1a.

There are a few features of the apparatus that are worthy of note. First, the laser system makes use of two commercial distributed

Bragg reflector (DBR) laser diodes; one diode drives the cooling transition while the other diode drives the repump transition. A tapered amplifier is used to ensure there is sufficient power available on the cooling transition, and acousto-optic modulators are used to prepare and control the beams required for the fountain sequence. The use of DBR laser diodes allows the laser system to be relatively simple, but this comes at the cost of increased laser frequency noise that can limit the achievable signal to noise ratio (Biedermann et al., 2009).

Second, the microwave cavity assembly makes use of a relatively simple feed structure compared to other microwave cavities developed for NIST fountains (Jefferts et al., 1998). NIST-F3 includes two cylindrical TE_{011} microwave cavities, one for state selection and one for the Ramsey interrogation of the clock transition. Both cavities have the same geometry. The radius is $R = 3$ cm and the height is $h \approx 2.17$ cm. The cavity assembly is illustrated in Fig. 1b. The cavity assembly is made of aluminum (Al 6061 T6), which has conductivity $\sigma = 2.5 \times 10^7$ S/m, approximately a factor of 2.3 smaller than the conductivity of copper. Microwaves can be fed into each cavity by use of handmade loop antennas which are inserted into the upper endcap. For the Ramsey cavity, we measure a loaded quality factor, Q, of about 5×10^3 compared to a theoretical Q of approximately 14×10^3 for a weakly coupled cavity with this geometry and conductivity. The two feeds to the Ramsey cavity are asymmetric; one feed requires nearly 16 dB more microwave power to drive the atomic resonance. This is illustrated in Fig. 1c with measurements of the Rabi oscillations as a function of microwave amplitude for the two feeds. The asymmetry in the feeds is not an inherent feature of the cavity design; a possible source of the asymmetry is a small, unintended movement of one feed during the final cavity assembly and bakeout. These features enhance NIST-F3's sensitivity to DCP errors (Li and Gibble, 2004, 2010). The lower conductivity of aluminum increases the DCP biases by a factor of approximately 1.5 compared to a copper cavity with the same geometry (Li and Gibble, 2010). The effects of the asymmetric cavity feeds are discussed in more detail in the next section.

A typical measurement of the short-term frequency stability of NIST-F3 is shown in Fig. 1d. In order to measure the collisional shift, we modulate the atom number by varying the loading time of the optical molasses. The detected atom number varies by approximately a factor of four between high-density and low-density mode. With the fountain operating in high-density mode, we measure a fractional frequency stability of $2.2 \times 10^{-13}/\sqrt{\tau}$. In low-density mode, we measure a stability of $4.0 \times 10^{-13}/\sqrt{\tau}$. The limitations to the short-term frequency stability in NIST-F3 are currently under investigation.

III. FREQUENCY BIASES

In most cesium fountains, the four largest frequency biases are the quadratic Zeeman shift due to the magnetic field used to lift the degeneracy between the atom's magnetic sub-levels, the BBR shift caused by the atoms interacting with the thermal radiation field, the collisional shift caused by the cold atoms interacting with each other, and the gravitational red shift that depends on where the fountain is located. Alongside these biases, there is a significant number of other shifts which must be considered, but these biases typically have a magnitude less than 1×10^{-15} in fractional frequency assuming the fountain is healthy (Guéna et al., 2012; Levi et al., 2014; Heavner et al., 2014; Szymaniec et al., 2016; Weyers et al., 2018; Beattie et al., 2020).

Although we are not aiming to achieve state of the art accuracy with NIST-F3, it is still important to monitor frequency biases that can vary in time like the quadratic Zeeman shift, the BBR shift, and the collisional shift to realize our frequency stability goals. It is also useful to correct the fountain for large, but relatively stable biases like the gravitational red shift. The quadratic Zeeman shift is determined by the magnetic field seen by the atoms inside the vacuum chamber. This magnetic field can be measured experimentally by driving a magnetically sensitive atomic transition, and the measured field can be used to calculate the bias on the clock transition (Wynands and Weyers, 2005). The BBR shift can be accurately calculated provided the temperature of the apparatus is known (Beloy et al., 2006; Angstmann et al., 2006; Safronova et al., 2010). The collisional shift can be measured by varying the launched atom number (Wynands and Weyers, 2005). The gravitational red shift is known from geodetic surveys of the clock labs at NIST Boulder (Pavlis and Weiss, 2017; McGrew et al., 2018). Typical values for these four biases are summarized in Table 1 along with conservative estimates of the uncertainty.

Once the known shifts have been corrected, we can estimate the size of the remaining frequency biases by comparing NIST-F3's frequency offset to one of NIST's local timescales or to the ensemble of primary and secondary frequency standards (PSFS) via Circular T. During our initial characterization, we discovered a large frequency bias of order 10^{-14} after correcting for the four biases summarized in Table 1. Subsequent investigations revealed that this bias was a first-order Doppler shift caused by a tilt in the atom's launch velocity with respect to gravity combined with an incorrect balance of the two feeds for the Ramsey cavity. The physics underlying this bias can be understood intuitively (Khursheed et al., 1996; Li and Gibble, 2010; Guéna et al., 2011). When the two feeds are incorrectly balanced, there is a transverse phase gradient in the Ramsey cavity. In this case, the cold-atom cloud will experience a different average phase each time the atoms cross the cavity if the atom's launch velocity is tilted with respect to gravity. This phase shift produces a frequency bias in the Ramsey interrogation.

In order to quantify this bias, it is useful to measure the fountain's frequency offset as a function of both the launch angle and the feed configuration (Guéna et al., 2011). The results are shown in Fig. 2a. We observe single-feed tilt sensitivities that are

Table 1: Typical values for the frequency biases that we routinely monitor in fractional frequency units. These four shifts are believed to be the largest fountain biases, assuming the fountain tilt sensitivity is well cancelled. The quadratic Zeeman shift corresponds to a magnetic field of approximately 212 nT. The uncertainty for the quadratic Zeeman shift corresponds to ± 1 fringe in the magnetically sensitive Ramsey spectroscopy. The position of any particular fringe can be measured with significantly better precision, but non-uniformities in the magnetic field seen by the atoms introduce uncertainty into the identification of the central fringe (Jefferts et al., 2002; Heavner et al., 2005). The value for the gravitational red shift was determined from geodetic surveys of the NIST clock labs with a correction for the height of the atoms in the fountain (Pavlis and Weiss, 2017; McGrew et al., 2018). The uncertainty given for the gravitational red shift corresponds to 1 m in the height of the atoms. The value for the BBR shift is calculated from the measured temperature of the apparatus. The temperature is measured by use of a platinum resistance temperature detector (RTD) mounted inside the vacuum chamber. The uncertainty given for the black body shift corresponds to 1 K due to uncertainty in the calibration of the RTD. The value given for the collisional shift was obtained by averaging six independent measurements of the collisional shift. The bias given is for the fountain operating in high-density mode. The uncertainty was estimated as the standard deviation of six independent measurements of the collisional shift. Over these six measurements, the atom number varies by approximately 10%. The scatter in the collisional shift measurements is comparable to the statistical uncertainty expected from the measured short-term stability.

Shift	Typical Value $(\times 10^{-15})$	Estimated Uncertainty $(\times 10^{-15})$
Quadratic Zeeman Shift	208.7	0.7
Gravitational Red Shift	180.9	0.1
Black Body Radiation Shift	-15.6	0.3
Collisional Shift	-2.1	0.7

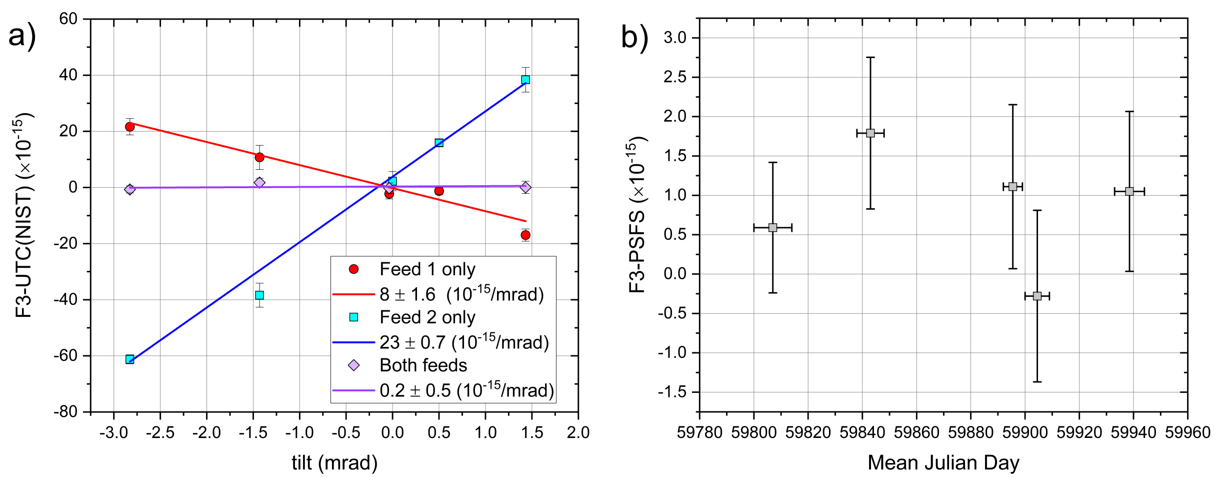

Figure 2: a) Measurements of NIST-F3's frequency offset vs tilt for three configurations of the microwave feeds. The fountain apparatus is tilted by adjusting the feet of the platform supporting the vacuum system shown in Fig. 1a. The tilting axis is approximately aligned with the axis connecting the feeds. The labels "Feed 1" and "Feed 2" are the same as in Fig. 1c. Solid lines are linear fits to the data. The magnitude of the best fit slope is given in the legend. b) Measurements of NIST-F3's frequency offset from PSFS over five months after applying the corrections summarized in Table 1. Horizontal error bars indicate the duration of each measurement campaign. Vertical error bars are a quadratic sum of the statistical uncertainty, the dead time uncertainty, and the time transfer uncertainty. The quadratic Zeeman shift, the BBR shift, and the collisional shift are measured in each campaign. The quadratic Zeeman shift is monitored while the fountain is running by interleaving measurements of the magnetically sensitive transition. The BBR shift is monitored by measuring the apparatus temperature. The collisional shift is determined by alternately running the fountain in high and low density modes.

asymmetric and of order $10^{-14}/\mathrm{mrad}$. NIST-F3's tilt sensitivity is enhanced by the relatively low conductivity of the cavity and by the strong coupling of the cavity feeds. The asymmetric tilt sensitivity is consistent with two feeds that have asymmetric coupling to the cavity (Li and Gibble, 2010). Even in the case of asymmetric coupling to the cavity, one expects that it is still possible to find a configuration with both feeds active where the transverse phase gradient is cancelled and the fountain has minimal tilt sensitivity. As Fig. 2a shows, we have achieved a configuration where the tilt sensitivity of the fountain with both feeds active is less than $1 \times 10^{-15}/\mathrm{mrad}$. Empirically, we found that this required the weakly coupled feed ("Feed 2" in Fig. 1c and Fig. 2a) to supply approximately 0.3 of the pulse area used to drive the atoms while the rest of the pulse area is supplied by the opposite feed.

The small measured tilt sensitivity in Fig. 2a is encouraging, but one has to be concerned that the apparatus might drift away from this configuration and develop a frequency bias. We routinely check that the fountain is well aligned vertically by comparing measurements with the fountain driven from the individual feeds and with both feeds. We also check for tilt sensitivity with both feeds operational. Over the last five months where F3 has been operating consistently, it appears possible to keep this shift suppressed at a level sufficient for our frequency stability goals.

To evaluate the long-term stability of NIST-F3, we compare the fountain to the PSFS ensemble via Circular T. Measurements of NIST-F3's offset relative to PSFS over five months are shown in Fig. 2b with corrections applied for the shifts in Table 1. The weighted average of these measurements gives an offset $\mathrm{F3} - \mathrm{PSFS} \approx (0.9 \pm 0.4) \times 10^{-15}$. The quadratic sum of the uncertainties given in Table 1 is 1×10^{-15}. A linear fit to the data gives a drift rate of $-1 \pm 6 \times 10^{-18}/\mathrm{day}$.

IV. CONCLUSION

NIST-F3 is now operating reliably, and we have completed an initial evaluation of the largest systematic biases. We are currently working to upgrade the apparatus and to investigate the residual frequency bias found in this first measurement campaign. Looking out further, we believe NIST-F3 will achieve its stability goals and begin contributing to the NIST time scale and the evaluation of NIST's frequency standards.

ACKNOWLEDGEMENTS

We gratefully acknowledge support from Stephan Barlow, Josh Savory, and Tom Heavner in the development of NIST-F3.

REFERENCES

Angstmann, E. J., Dzuba, V. A., and Flambaum, V. V. (2006). Frequency shift of hyperfine transitions due to blackbody radiation. *Phys. Rev. A*, 74:023405.

Bauch, A., Weyers, S., Piester, D., Staliuniene, E., and Yang, W. (2012). Generation of UTC(PTB) as a fountain-clock based time scale. *Metrologia*, 49(3):180.

Beattie, S., Jian, B., Alcock, J., Gertsvolf, M., Hendricks, R., Szymaniec, K., and Gibble, K. (2020). First accuracy evaluation of the NRC-FCs2 primary frequency standard. *Metrologia*, 57(3):035010.

Beloy, K., Safronova, U. I., and Derevianko, A. (2006). High-accuracy calculation of the blackbody radiation shift in the $^{133}\mathrm{Cs}$ primary frequency standard. *Phys. Rev. Lett.*, 97:040801.

Biedermann, G. W., Wu, X., Deslauriers, L., Takase, K., and Kasevich, M. A. (2009). Low-noise simultaneous fluorescence detection of two atomic states. *Opt. Lett.*, 34(3):347–349.

Guéna, J., Abgrall, M., Rovera, D., Laurent, P., Chupin, B., Lours, M., Santarelli, G., Rosenbusch, P., Tobar, M. E., Li, R., Gibble, K., Clairon, A., and Bize, S. (2012). Progress in atomic fountains at LNE-SYRTE. *IEEE Transactions on Ultrasonics, Ferroelectrics, and Frequency Control*, 59(3):391–409.

Guéna, J., Li, R., Gibble, K., Bize, S., and Clairon, A. (2011). Evaluation of doppler shifts to improve the accuracy of primary atomic fountain clocks. *Phys. Rev. Lett.*, 106:130801.

Hachisu, H., Nakagawa, F., Hanado, Y., and Ido, T. (2018). Months-long real-time generation of a time scale based on an optical clock. *Scientific Reports*, 8:4243.

Heavner, T. P., Donley, E. A., Levi, F., Costanzo, G., Parker, T. E., Shirley, J. H., Ashby, N., Barlow, S., and Jefferts, S. R. (2014). First accuracy evaluation of NIST-F2. *Metrologia*, 51(3):174.

Heavner, T. P., Jefferts, S. R., Donley, E. A., Shirley, J. H., and Parker, T. E. (2005). Recent improvements in NIST-F1 and a resulting accuracy of $\delta f/f = 0.61 \times 10^{-15}$. *IEEE Transactions on Instrumentation and Measurement*, 54(2):842–845.

Jefferts, S. R., Drullinger, R. E., and DeMarchi, A. (1998). NIST cesium fountain microwave cavities. In *Proceedings of the 1998 IEEE International Frequency Control Symposium (Cat. No.98CH36165)*, pages 6–8.

Jefferts, S. R., Shirley, J., Parker, T. E., Heavner, T. P., Meekhof, D. M., Nelson, C., Levi, F., Costanzo, G., DeMarchi, A., Drullinger, R., .Hollberg, L., Lee, W. D., and Walls, F. L. (2002). Accuracy evaluation of NIST-F1. *Metrologia*, 39(4):321.

Khursheed, A., Vecchi, G., and De Marchi, A. (1996). Spatial variations of field polarization and phase in microwave cavities: application to the cesium fountain cavity. *IEEE Transactions on Ultrasonics, Ferroelectrics, and Frequency Control*, 43(2):201–210.

Levi, F., Calonico, D., Calosso, C. E., Godone, A., Micalizio, S., and Costanzo, G. A. (2014). Accuracy evaluation of ITCsF2: a nitrogen cooled caesium fountain. *Metrologia*, 51(3):270.

Li, R. and Gibble, K. (2004). Phase variations in microwave cavities for atomic clocks. *Metrologia*, 41(6):376.

Li, R. and Gibble, K. (2010). Evaluating and minimizing distributed cavity phase errors in atomic clocks. *Metrologia*, 47(5):534.

McGrew, W. F., Zhang, X., Fasano, R. J., Schäffer, S. A., Beloy, K., Nicolodi, D., Brown, R. C., Hinkley, N., Milani, G., Schioppo, M., Yoon, T. H., and Ludlow, A. D. (2018). Atomic clock performance enabling geodesy below the centimetre level. *Nature*, 564:87–90.

Pavlis, N. K. and Weiss, M. A. (2017). A re-evaluation of the relativistic redshift on frequency standards at NIST, Boulder, Colorado, USA. *Metrologia*, 54(4):535.

Peil, S., Hanssen, J., Swanson, T. B., Taylor, J., and Ekstrom, C. R. (2016). The USNO rubidium fountains. *Journal of Physics: Conference Series*, 723(1):012004.

Rovera, G. D., Bize, S., Chupin, B., Guéna, J., Laurent, P., Rosenbusch, P., Uhrich, P., and Abgrall, M. (2016). UTC(OP) based on LNE-SYRTE atomic fountain primary frequency standards. *Metrologia*, 53(3):S81.

Safronova, M. S., Jiang, D., Arora, B., Clark, C. W., Kozlov, M. G., Safronova, U. I., and Johnson, W. R. (2010). Black-body radiation shifts and theoretical contributions to atomic clock research. *IEEE Transactions on Ultrasonics, Ferroelectrics, and Frequency Control*, 57(1):94–105.

Szymaniec, K., Lea, S. N., Gibble, K., Park, S. E., Liu, K., and Glowacki, P. (2016). NPL Cs fountain frequency standards and the quest for the ultimate accuracy. *Journal of Physics: Conference Series*, 723(1):012003.

Weyers, S., Gerginov, V., Kazda, M., Rahm, J., Lipphardt, B., Dobrev, G., and Gibble, K. (2018). Advances in the accuracy, stability, and reliability of the PTB primary fountain clocks. *Metrologia*, 55(6):789.

Wynands, R. and Weyers, S. (2005). Atomic fountain clocks. *Metrologia*, 42(3):S64.